JOURNAL OF MATERIALS SCIENCE **38** (2003) 833–841

Mixed alkali effect in borate glasses—optical absorption studies in Ho^{3+} doped $x(Na_2O) \cdot (30 - x)(K_2O) \cdot 70(B_2O_3)$ glasses

Y. C. RATNAKARAM
Department of Physics, Sri Venkateswara University P. G. Centre, Kavali 524 201, India

R. P. SREEKANTH CHAKRADHAR, K. P. RAMESH
Department of Physics, Indian Institute of Science, Bangalore 560 012, India

J. L. RAO
Department of Physics, S. V. University, Tirupathi 517 502, India

J. RAMAKRISHNA
Department of Physics, Indian Institute of Science, Bangalore 560 012, India
E-mail: jr@physics.iisc.ernet.in

Mixed alkali effect (MAE) in $xNa_2O \cdot (30 - x)K_2O \cdot 70B_2O_3$ ($x = 5$, 10, 15, 20 and 25) glasses doped with $0.5Ho_2O_3$ has been investigated by measuring the optical properties of Ho^{3+}. From the optical absorption spectra, optical band gaps (E_{opt}) for both direct and indirect transitions have been calculated using Davis and Mott theory and are found to exhibit a minimum when the two alkalies are in equal concentration (due to mixed alkali effect). Spectroscopic parameters like Racah (E^1, E^2, E^3), spin-orbit (ξ_{4f}), configuration interaction (α, β) and Judd-Ofelt intensity parameters (Ω_2, Ω_4 and Ω_6) have been calculated as a function of x. Also radiative and non-radiative transition probabilities (A_T and W_{MPR}), radiative lifetimes (τ_R), branching ratios (β) and integrated absorption cross sections (Σ) have been obtained. The spectral profile of the hypersensitive transition has been correlated to the site symmetry of the rare earth ion. The trends observed in the intensity parameters, radiative lifetimes and stimulated emission cross sections as a function of x in these borate glasses have been discussed, keeping in view the mixed alkali effect.

1. Introduction

Alkali borate glasses constitute interesting systems because of several structural changes induced upon adding increasing amounts of alkali oxide to the B_2O_3 glass. Fused B_2O_3 is assumed to consist of boroxyl rings and BO_3 triangles and constitutes a random network composed of two-dimensional units. The existence of several structural groups containing both three and four coordinated borons (e.g. penta borate, tetra borate, tri borate and di borate groups) was first postulated by Krogh-Moe [1] and confirmed by comparison with IR spectra of crystalline sodium borate compounds. It was found that at high alkali contents the fraction of four coordinated borons decreases again and non-bridging oxygens (bonded only to a single boron atom) become the dominant species in the glass [2]. If, in an alkali borate glass, the alkali oxide is progressively substituted by another, it is found that the resistivity does not vary linearly but goes through a maximum when the two alkalies are present in approximately equal concentrations. This is commonly known as the mixed alkali effect (MAE) [3]. However, the MAE has not been much investigated in borate glasses. In particular optical and spectroscopic studies are meager but they could be important and useful in understanding the microscopic origin of MAE in glasses.

Rare earth ions are used as dopants in glassy materials. Since the first laser action at 2.0 μm from the Ho^{3+} doped $CaWO_3$ crystal [4], various crystals and glasses doped with Ho^{3+} have been investigated as potential 2.0 μm light sources for medical and chemical sensing applications [5–7]. Recently, various spectroscopic investigations and energy transfer studies of Ho^{3+} ions in different glass hosts have been reported by several authors [8–12]. In this work we present the results of our studies on Ho^{3+} ions in $xNa_2O \cdot (30 - x)K_2O \cdot 70B_2O_3$ (where $x = 5$, 10, 15, 20 and 25) glasses, keeping in view the effect of mixed alkalies on the optical properties of Ho^{3+}

*Author to whom correspondence should be addressed.

in these borate glasses. Various spectroscopic parameters like Racah (E^1, E^2 and E^3), spin-orbit (ξ_{4f}) and configuration interaction (α, β) have been deduced. Energy values (E) of the different excited levels and spectral intensities (f) of these transitions are reported. As the intensity of the hypersensitive transitions depends on the covalency, coordination geometry and charge transfer effects, we correlate the intensities of these transitions with the surrounding environment and its chemical bonding to the rare earth ion. Using the Judd-Ofelt intensity parameters (Ω_2, Ω_4 and Ω_6), radiative transition probabilities (A_{rad}), radiative lifetimes (τ_R), branching ratios (β) and integrated absorption cross sections (Σ) have been calculated.

Glasses of the composition $x\mathrm{Na_2O} \cdot (30-x)\mathrm{K_2O} \cdot 70\mathrm{B_2O_3}$ (where $x = 5$, 10, 15, 20 and 25) doped with $0.5\mathrm{Ho_2O_3}$ were prepared and the optical absorption measurements were made with a Hitachi U-3400 spectrophotometer. The density measurements were made by Archimedes method using xylene as the immersion liquid. The refractive index was measured with an Abbe refractometer and it was found to be about 1.5. The physical properties of the glasses have been obtained using standard formulae [13].

2. Theory

2.1. Optical band gaps

Optical band gaps for direct and indirect transitions can be obtained following Davis and Mott [14]. We have,

$$\alpha(\omega) = B(\hbar\omega - E_{opt})^n/\hbar\omega \tag{1}$$

where $\alpha(\omega)$ is the absorption coefficient, B is a constant and E_{opt} is the optical band gap. For direct transitions $n = 1/2$ and for indirect transitions $n = 2$. From the plots of $(\alpha\hbar\omega)^2$ and $(\alpha\hbar\omega)^{1/2}$ as a function of photon energy $\hbar\omega$, E_{opt} values can be obtained for direct and indirect transitions respectively. The respective values of E_{opt} are obtained by extrapolating to $(\alpha\hbar\omega)^2 = 0$ for direct transitions and $(\alpha\hbar\omega)^{1/2} = 0$ for indirect transitions.

2.2. Spectral analysis

The interactions primarily responsible for the free ion structure in trivalent rare earth ions are the coulomb interaction and the magnetic interaction which is a coupling between their spin and orbital angular momenta. Methods of Racah [15] are used to calculate the electrostatic interaction matrix elements. Wybourne [16] has calculated appropriate electrostatic and spin-orbit parameters using RS coupling scheme. Using the methods of Wong [17] and Taylor's series expansion and using the observed band energies as E_J , zero order energies E_{0J} and partial derivatives of the rare earth ion [18], the correction factors ΔE^k, $\Delta\xi_{4f}$, $\Delta\alpha$ and $\Delta\beta$ are evaluated by least squares fit methods. From the known free ion parameters E^{k0}, ξ^0_{4f}, α^0 and β^0, the parameters E^k, ξ_{4f}, α and β in the complex are determined. Using the correction factors ΔE^k, $\Delta\xi_{4f}$, $\Delta\alpha$ and $\Delta\beta$, E_{cal} values are obtained.

The spectral intensities of the absorption bands are estimated by measuring the areas under the absorption curves using the relation [19]

$$f_{exp} = 4.318 \times 10^{-9} \int \in(\nu)\, d\nu \tag{2}$$

where $\int \in(\nu)$ represents the area under the absorption curve. The molar absorptivity $\in(\nu)$ of the corresponding band at energy ν (cm^{-1}) under the integral is given by

$$\in(\nu) = A/cl \tag{3}$$

where A is the absorbance, c is the concentration of the lanthanide ion in mol/ltr and l is the optical path length.

The f-f transitions are predominantly electric dipole in nature [20]. The magnetic dipolar contributions are negligible and not considered. The theoretical oscillator strengths, f_{cal} of the electric dipole transitions, within the f^N configurations can be calculated using Judd-Ofelt [20, 21] theory, in terms of the three intensity parameters Ω_2, Ω_4 and Ω_6 using the relation

$$f_{cal}(J, J') = \frac{8\Pi^2 mc\nu}{3h(2J+1)} \frac{(n^2+2)^2}{9n} \times \sum_{\lambda=2,4,6} \Omega_\lambda |\langle (SLJ)||U^\lambda||(S'L'J')\rangle|^2 \tag{4}$$

$\Omega_\lambda$can also be written as

$$\Omega_\lambda = (2\lambda+1) \sum_{t,p} |A_{t,p}|^2 \Xi(t,\lambda)^2 (2t+1)^{-1} \tag{5}$$

where $A_{t,p}$ are components of the crystal field operator and depend on the symmetry of the crystal field around the Ho^{3+} ions and Ξ (t, λ) is a function of radial integrals and depends reciprocally on the energy separation of the $4f^{10}$ and $4f^9 5d^1$ configurations. The sum over λ includes only the even values 2, 4 and 6 whereas the sum over t includes only the odd values 1, 3 and 5.

$||U^\lambda||^2$represents the square of the matrix elements of the unit tensor operator U^λ connecting the initial and final states. The matrix elements are calculated in the intermediate coupling approximations [22]. Because of the electrostatic shielding of the 4f electrons by the closed 5p shell electrons, the matrix elements of the unit tensor operator between two energy manifolds in a given rare-earth ion do not vary significantly when it is incorporated in different hosts. Therefore, the squared reduced matrix elements $||U^\lambda||^2$computed for the LaF_3 crystal given by Carnall *et al.* [23] have been used in the calculations.

Substituting the 'f_{meas}' for 'f_{cal}' and using the squared reduced matrix elements, the three intensity parameters $\Omega_\lambda(\lambda = 2, 4$ and $6)$ are obtained. The three intensity parameters are characteristic of a given rare earth ion (in a given matrix) and are related to the radial wave functions of the states $4f^N$ and the admixing states $4f^{N-1}$ 5d or $4f^{N-1}$ 5g and the ligand field parameters that characterize the environmental field. Generally Ω_2 is an indicator of the covalency of metal ligand bond

and Ω_4 and Ω_6 parameters are related to the rigidity of the host matrix.

2.3. Radiative properties

The Ω_λ values thus obtained from the absorption measurements are used to calculate the radiative transition probabilities, radiative lifetimes of the excited states and branching ratios. The radiative transition probability $A_{\text{rad}}(aJ, bJ')$ for emission from an initial state aJ to a final ground state bJ' is given by [24]

$$A_{\text{rad}}(aJ, bJ') = \frac{64\Pi^4\nu^3}{3h(2J+1)c^3}\frac{n(n^2+2)^2}{9} \times \sum_{\lambda=2,4,6} \Omega_\lambda |\langle (SLJ)||U^\lambda||(S'L'J')\rangle|^2 \tag{6}$$

The total radiative emission probability $A_{\text{T}}(aJ)$ involving all the intermediate terms between aJ and bJ' is given by the sum of the $A_{\text{rad}}(aJ, bJ')$ terms calculated over all terminal states bJ'

$$A_{\text{T}}(aJ) = \sum_{bJ'} A_{\text{rad}}(aJ, bJ') \tag{7}$$

The radiative lifetime τ_{R}, of the emission state is

$$\tau_{\text{R}} = A_{\text{T}}(aJ)^{-1} \tag{8}$$

The fluorescence branching ratio β_{R} is defined as

$$\beta(aJ, bJ') = \frac{A(aJ, bJ')}{A_{\text{T}}(aJ)} \tag{9}$$

The integrated absorption cross section (Σ) for the stimulated emission is [25]

$$\Sigma = \frac{1}{\nu^2}\frac{A}{8\Pi cn^2} \tag{10}$$

3. Results and discussion

3.1. Optical band gaps

Optical band gap (E_{opt}) values are obtained for both indirect and direct transitions of Ho^{3+} doped mixed alkali borate glasses from the graphs of $(\alpha\hbar\omega)^{1/2}$ and $(\alpha\hbar\omega)^2$ versus $\hbar\omega$. These values are presented in Table I. Some of the physical properties are also presented in Table I

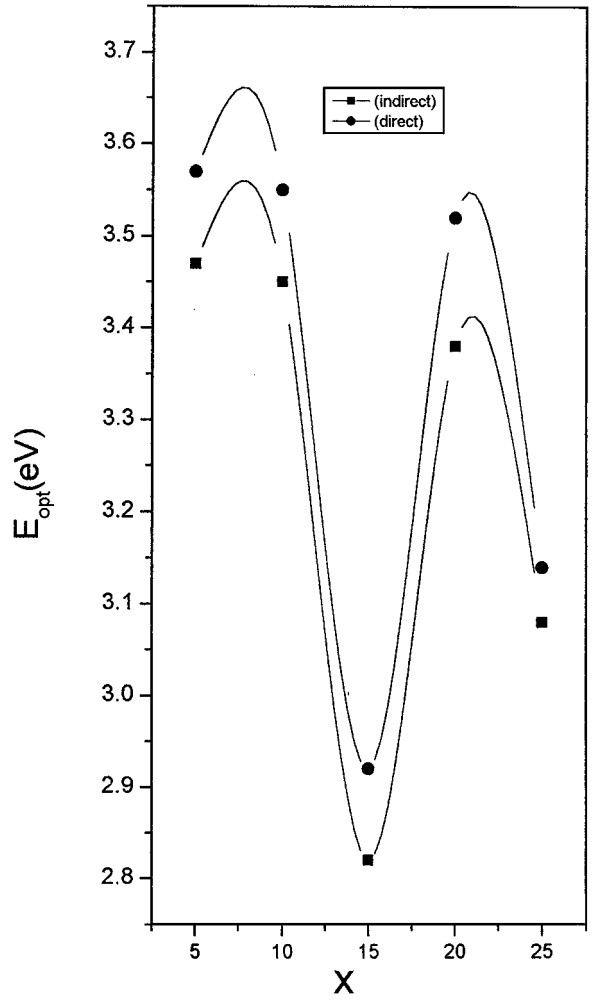

Figure 1 Variation of optical band gaps (E_{opt}) with x in $x\text{Na}_2\text{O} \cdot (30-x)\text{K}_2\text{O} \cdot 70\text{B}_2\text{O}_3$ glasses.

for all the glasses studied. Fig. 1 shows the variation of E_{opt} with x in the glass and it is observed that the optical band gap values exhibit a minimum for $x = 15$ i.e., when the two alkalies are present in equal concentrations. It may be due to increase in the covalency of Ho–O bonds (due to increase in the number of non-bridging oxygens).

3.2. Spectroscopic parameters

The electronic configuration of the Ho^{3+} ion is $4f^{10}$ and its ground state is $^5I_8$. Fig. 2 shows the optical absorption spectra of Ho^{3+} in all the mixed alkali

TABLE I Optical band gaps (E_{opt})(eV) and certain physical properties of Ho^{3+} doped $x\text{Na}_2\text{O} \cdot (30-x)\text{K}_2\text{O} \cdot 70\text{B}_2\text{O}_3$ glasses

S. no.	Property	Glass A ($x=5$)	Glass B ($x=10$)	Glass C ($x=15$)	Glass D ($x=20$)	Glass E ($x=25$)
1.	Optical bad gaps					
	(a) Direct transitions	3.57	3.55	2.92	3.52	3.14
	(b) Indirect transitions	3.47	3.45	2.82	3.38	3.08
2.	Average Molecular Weight (M, g)	84.711	83.101	81.489	79.879	78.267
3.	Density (d, g/cm^3)	2.976	2.548	2.540	2.602	2.826
4.	Refractive index (n)	1.506	1.506	1.505	1.506	1.507
5.	Concentration ($N \times 10^{-22}$, ions/cm^3)	1.058	0.923	0.939	0.981	1.087
6.	Polaron radius (r_{p}, A^0)	1.835	1.921	1.910	1.882	1.819
7.	Interionic distance (r_{I}, A^0)	4.555	4.767	4.739	4.671	4.514
8.	Field strength ($F \times 10^{-16}$, cm^2)	0.891	0.813	0.822	0.847	0.906

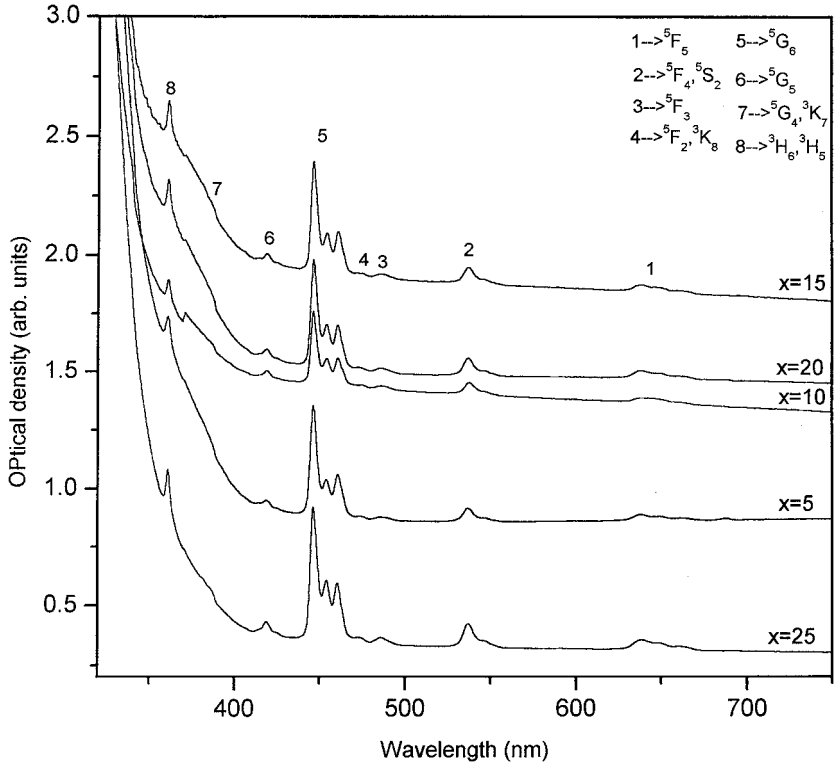

Figure 2 Optical absorption spectra of Ho^{3+} in $xNa_2O \cdot (30 - x)K_2O \cdot 70B_2O_3$ glasses.

borate glasses studied at room temperature in the UV-VIS range. The experimental and calculated energies of all the excited levels of Ho^{3+} ion, along with their assignments are presented in Table II. From the table it is observed that a full matrix diagonalization procedure leads to a good fit between the observed and calculated energies as shown by small rms deviations. The Racah (E^1, E^2 and E^3), spin-orbit (ξ_{4f}) and configuration interaction (α, β) parameters obtained for all the glasses are also presented in Table II. The hydrogenic ratios E^1/E^3 and E^2/E^3, which are related to the radial properties of Ho^{3+}, are more or less same for all the mixed alkali borate glasses, which means that radial properties are not much affected by the presence of mixed alkalies.

3.3. Spectral intensities and intensity parameters

The experimental (f_{exp}) and calculated (f_{cal}) spectral intensities (using Judd-Ofelt intensity parameters) of Ho^{3+} ion in all the mixed alkali borate glasses are presented in Table III along with their rms deviation values. The rms deviation between experimental and calculated values is very low confirming the validity of Judd-Ofelt theory. The maximum variation in intensities is ±20%

TABLE II Experimental (E_{exp}) and calculated (E_{cal}) energies and various spectroscopic parameters of Ho^{3+} doped $xNa_2O \cdot (30 - x)K_2O \cdot 70B_2O_3$ glasses (energy values are in cm^{-1})

		Glass A		Glass B		Glass C		Glass D		Glass E	
S. no.	Energy level	E_{exp}	E_{cal}	E_{exp}	E_{cal}	E_{exp}	E_{cal}	E_{exp}	E_{cal}	E_{exp}	E_{cal}
1.	$^5F_5$	15487	15512	15572	15572	15682	15675	15694	15682	15657	15655
2.	$^5F_4$, $^5S_2$	18582	18580	18599	18609	18617	18607	18634	18678	18634	18643
3.	$^5F_3$	20549	20575	20570	20567	20549	20537	20613	20595	20591	20588
4.	$^5F_2$, $^3K_8$	21091	21046	21069	21066	21091	21097	21158	21167	21158	21162
5.	$^5G_6$	22415	22404	22415	22413	22415	22416	22415	22415	22415	22415
6.	$^5G_5$	23888	23910	23859	23865	23859	23865	23888	23894	23888	23891
7.	$^5G_4$, $^3K_7$	25766	25752	25699	25698	–	–	–	–	–	–
8.	$^3H_6$, $^3H_5$	27693	27696	27693	27693	27693	27699	27693	27693	27693	27694
rms deviation			±45		±9		±20		±50		±11
	E^1		7081.4		7204.9		7199.6		7280.4		7359.1
	E^2		31.4		31.8		32.1		31.1		30.7
	E^3		696.5		703.6		695.4		707.7		717.7
	ξ_{4f}		2072.2		2039.3		1990.0		1994.5		1994.8
	α		105.7		115.8		103.8		120.1		133.9
	β		−2722.4		−3128.2		−3023.4		−3457.6		−3771.7
	E^1/E^3		10.16		10.24		10.35		10.30		10.25
	E^2/E^3		0.045		0.045		0.046		0.044		0.043

TABLE III Experimental and calculated spectral intensities ($f \times 10^6$) of Ho^{3+} doped $xNa_2O \cdot (30-x)K_2O \cdot 70B_2O_3$ glasses

S. no.	Energy level	Glass A		Glass B		Glass C		Glass D		Glass E	
		f_{exp}	f_{cal}	f_{exp}	f_{cal}	f_{exp}	f_{cal}	f_{exp}	f_{cal}	f_{exp}	f_{cal}
1.	$^5F_5$	0.895	1.258	3.488	3.744	3.372	3.958	3.951	3.687	0.880	3.123
2.	$^5F_4$,$^5S_2$	2.553	2.038	5.881	5.535	6.902	6.279	5.124	5.416	5.036	4.571
3.	$^5F_3$	0.716	0.754	1.467	1.914	1.781	2.392	1.870	1.872	1.451	1.570
4.	$^5F_2$,$^3K_8$	0.253	0.456	0.583	1.155	0.808	1.392	0.440	1.132	0.512	0.951
5.	$^5G_6$	22.551	22.219	39.667	39.645	42.791	42.750	44.456	44.584	42.611	42.451
6.	$^5G_5$	1.126	0.620	2.719	2.597	2.399	2.023	2.239	2.545	2.607	2.204
7.	$^5G_4$,$^3K_7$	–	–	2.276	0.823	–	–	–	–	1.500	0.725
8.	$^3H_6$,$^3H_5$	3.018	5.316	9.934	9.944	10.563	10.690	12.003	10.953	7.858	10.272
rms deviation			±1.233		±1.327		±0.633		±1.472		±1.191

TABLE IV Judd-Ofelt intensity parameters ($\Omega_\lambda \times 10^{20}$)($cm^2$) and peak intensity ratios (I_L/I_S) of hypersensitive transition ($^5G_6$) of Ho^{3+} in $xNa_2O \cdot (30-x)K_2O \cdot 70B_2O_3$ glasses

Parameter	Ω_2	Ω_4	Ω_6	$\Sigma\Omega_\lambda$	I_L/I_S (3, 1)	I_L/I_S (3, 2)	Ref.
$5Na_2O+25K_2O+70B_2O$	7.474	0.576	1.233	9.283	1.443	1.209	Present work
$10Na_2O+20K_2O+70B_2O_3$	12.235	2.416	3.123	17.774	1.782	1.815	Present work
$15Na_2O+15K_2O+70B_2O_3$	13.556	1.886	3.760	19.202	1.739	1.785	Present work
$20Na_2O+10K_2O+70B_2O_3$	13.998	2.365	3.048	19.411	2.000	1.923	Present work
$25Na_2O+5K_2O+70B_2O_3$	13.474	2.047	2.560	18.091	1.800	1.766	Present work
$30Na_2O+70B_2O_3$	5.30	2.52	1.53	9.35			[35]
$30K_2O+70B_2O_3$	5.29	1.40	0.78	7.47			[35]
$30Li_2O+70B_2O_3$	4.56	3.14	1.78	9.48			[35]
$30CaO+70B_2O_3$	4.90	3.29	1.74	9.93			[35]
$30BaO+70B_2O_3$	4.96	2.99	1.61	9.56			[35]
$81B_2O_3+10Na_2O+8LiF$	11.920	17.025	2.964	31.909			[36]
$81B_2O_3+10Na_2O+8NaF$	12.174	18.895	4.745	35.814			[36]

for most of the optical absorption bands from one glass to another. However, the intensities of the hypersensitive transitions ($^5G_6$ and $^3H_6$) change with glass composition. The intensities of these transitions are low in glasses with $x = 5$ and high in glasses with $x = 20$. It indicates that the crystal field asymmetry at the site of Ho^{3+} ion is low in the potassium rich glasses and high in the sodium rich glasses [26].

The Judd-Ofelt intensity parameters (Ω_2, Ω_4 and Ω_6) obtained from a least square analysis of the observed oscillator strengths for all the mixed alkali borate glasses studied are presented in Table IV. These parameters depend on the host glass composition [27]. It is known that the Judd-Ofelt parameter Ω_2 in particular, increase with increasing covalency of the bond between the rare earth ion and the ligand anions. Oomen and van Dongen [28] have suggested that, instead of observing the variation in Ω_2 alone, it is convenient to see the variation of the sum of the Judd-Ofelt parameters $\Sigma\Omega_\lambda$, which also increases with increasing covalency. In the present work, the variation of $\Sigma\Omega_\lambda$ and Ω_2 with x is similar (Fig. 3). The binary potassium borate glass exhibits relatively low values for Ω_4 and Ω_6 (low rigidity) and addition of a small quantity of sodium (5%) results in a small increase in the value of Ω_2 (compared to that in the binary glass) along with a small decrease in Ω_4 and Ω_6. On the other hand, addition of a small quantity of potassium (5%) to the binary sodium rich glass leads to a large increase in the value of Ω_2. But when the two alkalies are in comparable concentration ($x = 10$ to 20), the Ω_2 and $\Sigma\Omega_\lambda$ values do not change significantly, though a shallow minimum could be seen for $x = 15$ (equal concentrations) due to the mixed alkali effect.

According to Equation 5, the increase of Ω_2 with x can be due to an increase of the crystal field parameters $A_{t,p}$ (with odd t values) and/or increase of the

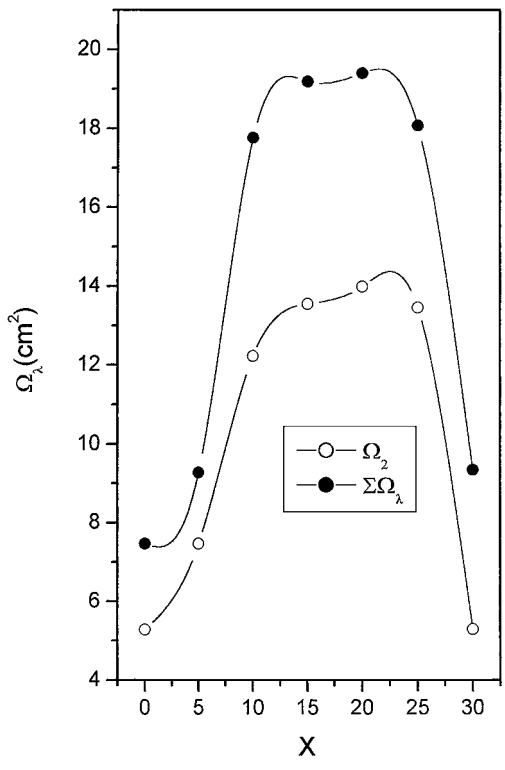

Figure 3 Variation of $\Omega_\lambda(\times 10^{20})$ and $\Sigma\Omega_\lambda(\times 10^{20})$ with x in $xNa_2O \cdot (30-x)K_2O \cdot 70B_2O_3$ glasses.

$\Xi(t,\lambda)$. An increase in the value of $\Xi(t,\lambda)$ would be produced by a decrease of the energy difference between the $4f^N$-states and the admixed configuration and/or by an increase of the corresponding radial integrals. Both these changes may be caused by an increase of the electron density on the oxygen ions [29, 30] which, on the other hand, should correlate with increasing covalency, according to the nephelauxetic effect [19]. Ω_6 is maximum when $x = 15$ in the glass matrix which indicates that rigidity of the host material is high when the two alkalies are present in equal concentration.

In Table IV, the Judd-Ofelt intensity parameters in mixed alkali borate glasses are compared with those in other binary borate glasses and ternary fluoride glasses. It is observed from the table that Ω_λ values are less in binary (for 30 mol% of either Na_2O or K_2O) glasses, which indicates that, with the addition of the second alkali, the covalence increases in these glasses. In the case of mixed ternary fluoride glasses, Ω_4 parameter is very high (indicating high rigidity), though Ω_2 and Ω_6 parameters are in the same order as in the mixed alkali oxide glasses. Hence $\Sigma\Omega_\lambda$ values turn out to be much more when compared with binary borate glasses.

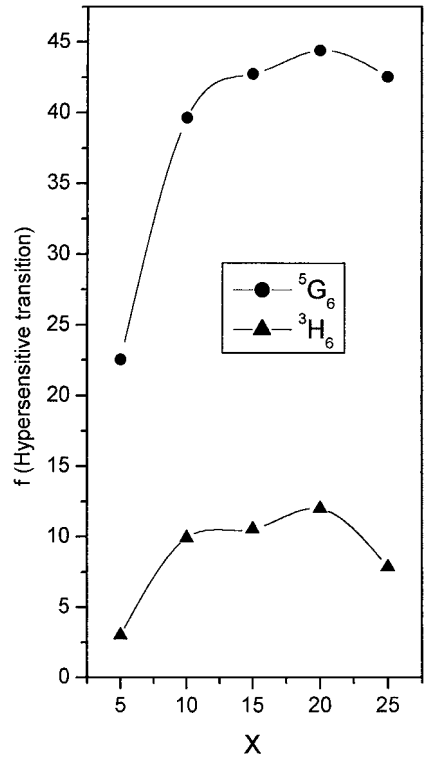

Figure 4 Variation of intensity of the hypersensitive transition ($f \times 10^6$) with x in $x Na_2O \cdot (30-x)K_2O \cdot 70B_2O_3$ glasses.

3.4. Hypersensitive transitions

$^5I_8 \rightarrow {}^3H_6$ and $^5I_8 \rightarrow {}^5G_6$ are the hypersensitive transitions for Ho^{3+} ion [24]. These transitions will obey the selection rules $\Delta L \leq 0$, $\Delta J \leq 0$ and $\Delta S = 0$ and they are sensitive to the environment. Generally, Ω_2 parameter which indicates covalency, increases or decreases with the intensity of the hypersensitive transition [24]. In the present work, except for the intensity of the $^3H_6$ band of $x = 25$, Ω_2 parameter decreases with the decreasing intensity of the hypersensitive transition. The shift of the peak wavelength of the hypersensitive transition towards longer wavelengths with an increase of alkali content, indicates that the degree of covalency of R—O bond increases with alkali content. In the present work, there is no shift in the peak wavelengths of the hypersensitive transitions. This may be due to the fact the total alkali content is constant and the relative concentration of Na_2O and K_2O may not sufficiently affect the Ho—O bond to shift the hypersensitive transition. The intensities of the hypersensitive transitions increase with x, but for $x = 25$ it decreases. Fig. 4 shows the variation of intensity of the hypersensitive transitions with x. Here also there is small dip at $x = 15$ which indicates the mixed alkali effect.

The hypersensitive transition, $^5I_8 \rightarrow {}^5G_6$ in all the absorption spectra of Ho^{3+} doped glasses is split into three sharp peaks by the Stark splitting due to the crystal field. The peak to peak separation is the same in all the mixed alkali borate glasses studied. The relative intensity ratio between the peaks I_L/I_S, where I_L is the intensity of the peak with longer wavelength and I_S is the intensity of the peak with shorter wavelength, varies with glass composition. The variation of peak intensity ratios (I_L/I_S) with x is similar for (3,1) and (3,2) peaks. The I_L/I_S values are presented in Table IV. Variation of I_L/I_S with x is shown in Fig. 5. I_L/I_S for (3,1) and (3,2) show a shallow

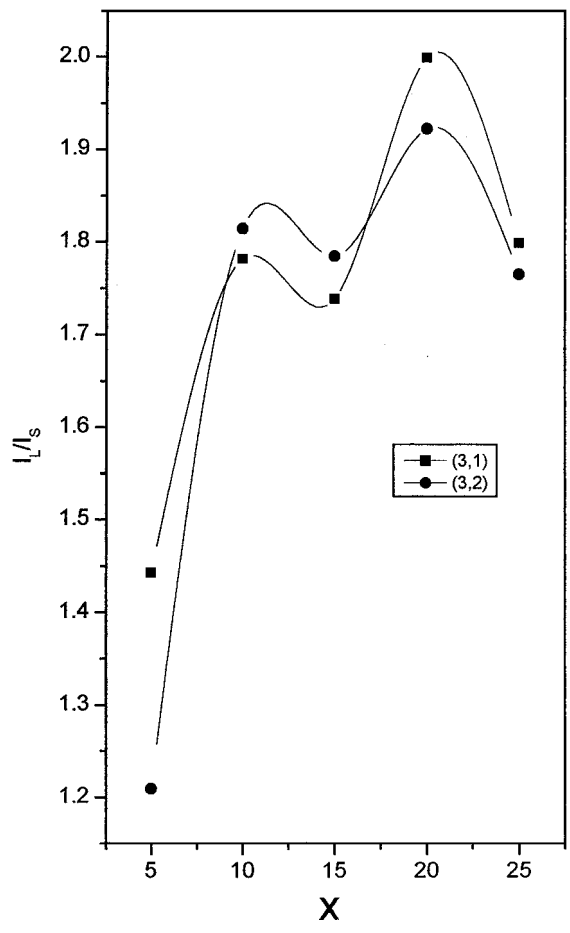

Figure 5 Variation of peak intensity ratios (I_L/I_S) with x in $x Na_2O \cdot (30-x)K_2O \cdot 70B_2O_3$ glasses.

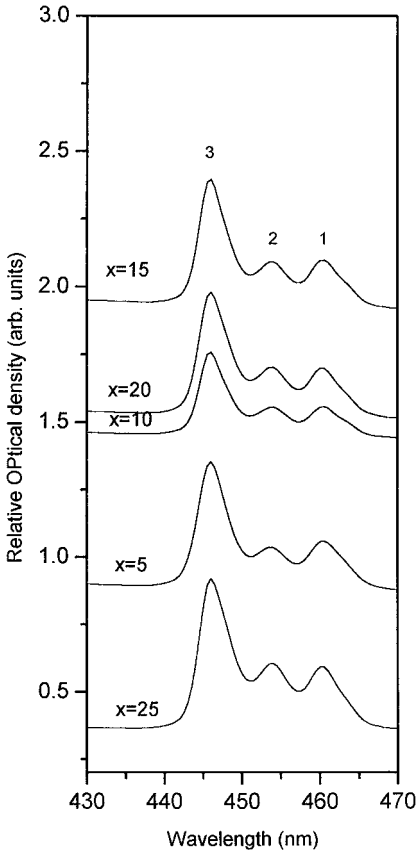

Figure 6 Variation of spectral profile of the hypersensitive transition ($^5I_8 \rightarrow {}^5G_6$) with x in $xNa_2O \cdot (30-x)K_2O \cdot 70B_2O_3$ glasses.

minimum at $x = 15$ which may be due mixed alkali effect.

The spectral profile of hypersensitive transition ($^5I_8 \rightarrow {}^5G_6$) is shown in Fig. 6 for all the glasses studied. A difference in the shape of this transition indicates a difference in the environment of the Ho^{3+} ion i.e., it indicates changes in the symmetry of the crystalline field acting on the rare earth ion. The hypersensitive band structure consists of three sharp peaks (1,2,3). As x increases from 5 to 15, the height of peak 1 increases and the height of peak 2 decreases (relatively) which indicates that structural changes occur in the glass matrix for $x = 5$, 10 and 15. Intensity of peak 3 shows a maximum at $x = 15$. For $x = 20$ and 25, the spectral profile of hypersensitive transition does not change which shows that the surrounding environment (symmetry) is the same for these two glass systems. Sodium oxygens affect the crystal field more than the potassium oxygens and reach a saturation for $x = 20$.

3.5. Radiative and non-radiative transition rates

Using the Judd-Ofelt intensity parameters Ω_λ obtained from the measured oscillator strengths of the absorption bands, the total radiative transition rates (A_T) and radiative lifetimes (τ_R) for various excited states $^3H_4$, $^5G_6$, $^3K_8$, $^5F_2$, $^5F_3$ and $^5F_4$ of the Ho^{3+} ion have been calculated using Equations 7 and 8 and are presented in Table V. It is observed that the lifetimes of all the excited states decrease (i.e., A_T increases) up to $x = 15$ (for $^3H_5$ and $^5G_6$ states up to $x = 20$) and for $x = 20$ and 25 lifetimes slightly increases. In all the mixed alkali borate glasses, lifetimes for the different levels obey the same trend viz., $^3K_8 > {}^5F_2 > {}^5F_4 > {}^5F_3 > {}^3H_5 > {}^5G_6$. We have calculated the radiative transition rates directly from the measured oscillator strengths for the $^5G_6 \rightarrow {}^5I_8$ and $^5F_4 \rightarrow {}^5I_8$ transitions in all the mixed alkali borate glasses using the relation [31]

$$A'_{JJ} = \frac{8\pi^2 e^2 n^2 \nu^2}{mc} \frac{2J'+1}{2J+1} f'_{JJ} \qquad (11)$$

where J and J' represent the $^5G_6$, $^5F_4$ and $^5I_8$ levels respectively (transition rates for the five glasses are 22523 sec^{-1}, 39555 sec^{-1}, 42740 sec^{-1}, 44403 sec^{-1} and 42560 sec^{-1} for $^5G_6 \rightarrow {}^5I_8$ transition and 2531 sec^{-1}, 5847 sec^{-1}, 6860 sec^{-1}, 5133 sec^{-1} and 5025 sec^{-1} for $^5F_4 \rightarrow {}^5I_8$ transition). These transition rates are in reasonable agreement with the values calculated by using Judd-Ofelt theory (Table V).

The exponential dependence of the multi-phonon relaxation rate W_{MPR} on the energy gap to the next lower level ΔE, has been experimentally established for a number of crystals and glasses and is given by [32]

$$W_{MPR} = C \exp(-\alpha \Delta E) \qquad (12)$$

where C and α are positive, host dependent constants, which are almost independent of the specific 4f level of trivalent rare-earth ions (except in a few cases). Using the above equation, non-radiative relaxation rate constants for the various Ho^{3+} excited states in mixed alkali borate glasses were calculated using the values of $\alpha = 3.8 \times 10^{-3}$ cm^{-1} and $C = 2.9 \times 10^{12}$ sec^{-1} reported for borate glasses [33]. The predicted non-radiative relaxation rates for the observed excited state multiplets are presented in Table VI for $x = 5$, 15 and 25 (for the other compositions, ΔE values are in the same range) in the glass matrix. It is observed that non-radiative

TABLE V Total radiative transition probabilities (A_T)(sec^{-1}) and radiative lifetimes (τ_R)(μs) of certain excited states of Ho^{3+} in $xNa_2O \cdot (30-x)K_2O \cdot 70B_2O_3$ glasses

		Glass A		Glass B		Glass C		Glass D		Glass E	
S. no.	Excited level	A_T	τ_R	A_T	τ_R	A_T	τ_R	A_T	τ_R	A_T	τ_R
1.	$^3H_5$	16468	60	30384	33	33377	30	34174	29	32242	31
2.	$^5G_6$	24775	40	44314	22	47713	21	49635	20	47103	21
3.	$^3K_8$	488	2049	1070	934	1192	839	1078	927	954	1047
4.	$^5F_2$	1744	573	4698	213	5563	179	4766	210	4021	248
5.	$^5F_3$	2055	486	5684	176	6439	155	5680	176	4803	208
6.	$^5F_4$	1912	523	5464	183	6036	165	5444	183	4600	217

TABLE VI Calculated non-radiative relaxation rates (W_{MPR})(S^{-1}) for excited levels of Ho^{3+} in $xNa_2O \cdot (30-x)K_2O \cdot 70B_2O_3$ glasses (energy values are in cm^{-1})

		$x=5$		$x=15$		$x=25$	
S. no.	Excited level	ΔE	W_{MPR}	ΔE	W_{MPR}	ΔE	W_{MPR}
1.	$^5S_2$	2825	6.313×10^7	2932	4.203×10^7	3007	3.161×10^7
2.	$^5F_4$	243	1.151×10^{12}	27	2.617×10^{12}	19	2.698×10^{12}
3.	$^5F_3$	1995	1.479×10^9	1903	2.098×10^9	1945	1.788×10^9
4.	$^3K_8$	364	0.727×10^{12}	92	2.044×10^{12}	48	2.416×10^{12}
5.	$^5F_2$	107	1.931×10^{12}	468	0.489×10^{12}	526	0.392×10^{12}
6.	$^5G_6$	1358	0.016×10^{12}	1319	0.019×10^{12}	1254	0.024×10^{12}
7.	$^5G_5$	1506	9.484×10^9	1449	0.012×10^{12}	1475	0.011×10^{12}
8.	$^5G_4$	1842	2.645×10^9	1863	2.442×10^9	1725	4.126×10^9

TABLE VII Branching ratios (β) and integrated absorption cross sections ($\Sigma \times 10^{18} cm^{-1}$) of certain transitions of Ho^{3+} doped $xNa_2O \cdot (30-x)K_2O \cdot 70B_2O_3$ glasses

		Glass A		Glass B		Glass C		Glass D		Glass E	
S. no.	Transition	β	Σ	β	Σ	β	Σ	β	Σ	β	Σ
1.	$^3H_5 \rightarrow {}^5I_7$	0.797	14.57	0.744	24.89	0.754	27.37	0.761	28.33	0.772	27.1
2.	$^5G_6 \rightarrow {}^5I_8$	0.909	26.13	0.892	45.82	0.894	49.41	0.896	51.53	0.889	49.07
3.	$^3K_8 \rightarrow {}^5I_8$	0.886	0.57	0.883	1.27	0.880	1.43	0.882	1.30	0.885	1.15
4.	$^5F_2 \rightarrow {}^5I_8$	0.598	1.37	0.563	3.47	0.575	4.18	0.550	3.40	0.547	2.86
5.	$^5F_3 \rightarrow {}^5I_8$	0.574	1.62	0.525	4.11	0.556	4.94	0.515	4.01	0.511	3.37
6.	$^5F_4 \rightarrow {}^5I_8$	0.838	2.70	0.812	7.45	0.823	8.33	0.802	7.30	0.800	6.16

decay rate is the dominant relaxation process for all the excited levels of Ho^{3+} in borate glasses.

As mentioned earlier, we have calculated the energy values of the excited levels of Ho^{3+} ion and we find that the energy level separation between $^5F_2$ and $^3K_8$ transitions is very small ($107\ cm^{-1}$) in the case of $x = 5$ in the glass matrix. For the other compositions i.e., $x = 10, 15$, 20 and 25, the energy level separation between $^3K_8$ and $^5F_3$ is much less i.e., $211\ cm^{-1}$, $92\ cm^{-1}$, $32\ cm^{-1}$, and $48\ cm^{-1}$ respectively. Thus at room temperature thermalization for the two levels occurs and the effective radiative transition probabilities A_{eff} can be calculated using the relation [34].

$$A_{eff} = \frac{12\exp[-\Delta E/KT]\Sigma A\left({}^5F_2/{}^3K_8\right) + 4\Sigma A\left({}^3K_8/{}^5F_3\right)}{12\exp[-\Delta E/KT] + 4} \quad (13)$$

where $KT = 209\ cm^{-1}$ and ΣA is the total radiative transition rates (Table V). The effective transition rates for the above transitions in these glasses are $3555\ sec^{-1}$, $3274\ sec^{-1}$, $2981\ sec^{-1}$, $2365\ sec^{-1}$ and $2091\ sec^{-1}$.

The variation of A_T values with x is shown in Fig. 7. The branching ratios (β) and integrated absorption cross sections (Σ) for certain transitions are collected in Table VII. It is observed that branching ratios for the transitions $^3H_5 \rightarrow {}^5I_7$, $^5G_6 \rightarrow {}^5I_8$ and $^3K_8 \rightarrow {}^5I_8$ are high in glasses where $x = 25$ in the glass matrix and for $x = 15$, the branching ratio is high for $^5F_2 \rightarrow {}^5I_8$, $^5F_3 \rightarrow {}^5I_8$ and $^5F_4 \rightarrow {}^5I_8$ transitions. The integrated absorption cross sections (Σ) are high for $^3H_5 \rightarrow {}^5I_7$ and $^5G_6 \rightarrow {}^5I_8$ transitions in the case of $x = 20$ in the glass matrix. Hence these transitions could be useful for laser excitation.

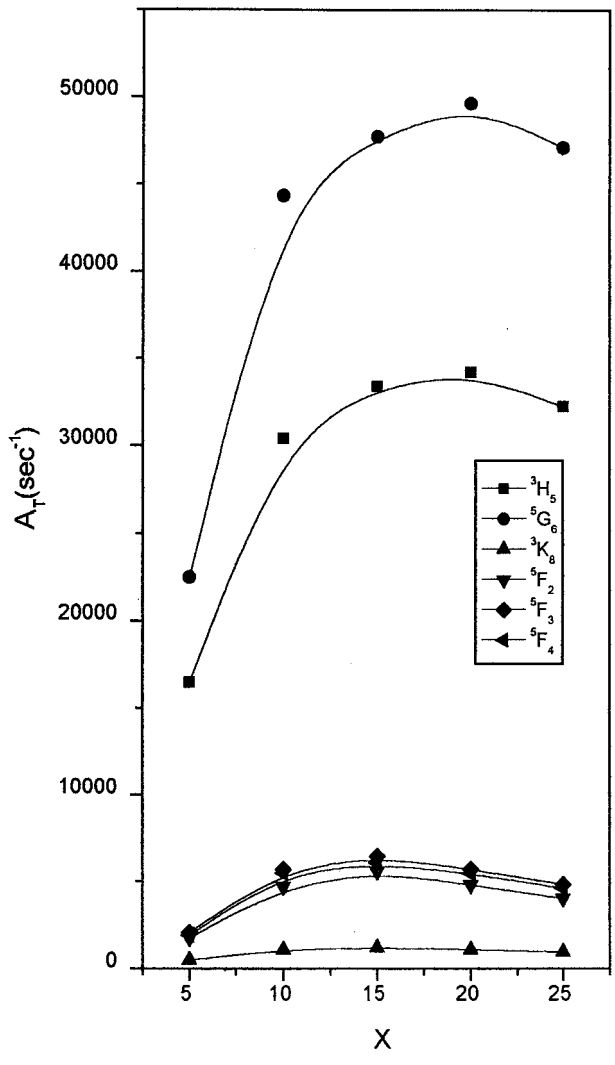

Figure 7 Variation of total radiative transition probabilities (A_T)(s^{-1}) with x in $xNa_2O \cdot (30-x)K_2O \cdot 70B_2O_3$ glasses.

4. Conclusions

The optical band gaps (E_{opt}) for both direct and indirect transitions exhibit a minimum in the mixed alkali borate glasses when the two alkalies are in equal concentrations. The Judd-Ofelt theory works well for the Ho^{3+} ion in all the mixed alkali borate glasses studied. The Judd-Ofelt parameters, in particular Ω_2, are greater in mixed alkali borate glasses than in the corresponding binary borate glasses. The higher values of Ω_2 indicate higher covalency between holmium cation and oxide anions. The intensity parameter Ω_2 and the sum of the intensity parameters $\Sigma\Omega_\lambda$ show a small dip at $x = 15$, i.e., at equal concentrations of K_2O and Na_2O, due to the mixed alkali effect. The mixed alkali effect is seen in the variation of intensities of the hypersensitive transitions with alkali content in the glass. The radiative transition probabilities, radiative lifetimes, branching ratios and integrated absorption cross sections are calculated for certain excited states and some of the potential lasing transitions are identified.

Acknowledgements

Y.C.R expresses his thanks to the Head, Department of Physics, S. V. U. P. G. Centre, Kavali for his support in the execution of the above work and R. P. S. Chakradhar is grateful to SERC (DST), New Delhi for financial assistance.

References

1. J. KROGH-MOE, *Phys. Chem. Glasses* **3** (1962) 101.
2. P. J. BRAY and J. G. O'KEEFE, *ibid.* **4** (1963) 37.
3. A. PAUL, "Chemistry of Glasses," 2nd ed. (Chapman and Hall, New York, 1990) 10001.
4. L. J. JOHNSON, G. D. BOYD and K. NASSAU, in Proc. IRE, Vol. 50 (1962), 87.
5. H. HEMMATI, *Opt. Lett*. **14**(9) (1989) 435.
6. E. W. DUCZYNSKI and G. HUBER, *Appl. Phys. Lett.* **48**(23) (1986) 1562.
7. Ch. GHISLER, W. LUTHY, H. P. WEBER, J. MOREL, A. WOODTLI, R. DANDLIKER, V. NEUMAN, H. BERTHOU and G. KOTROTSIOS, *Opt. Commun*. **109** (1994) 279.
8. K. BINNEMANS, R. VAN DEUN, C. GORLLER-WALRAND and J. L. ADAM, *J. Non-Cryst. Solids* **238** (1998) 11.
9. P. NACHIMUTHU and R. JAGANNADHAN, *J. Amer. Ceram. Soc.* **82**(2) (1999) 387.
10. Y. B. SHIN, H. T. LIM, Y. G. CHOI, Y. S. KIM and J. HEO, *ibid.* **83**(4) (2000) 787.
11. M. WACHTLER, A. SPEGHINI, K. GATTERER, H. P. FRITZER, DAVID AJO and M. BETTINELLI, *ibid.* **81**(8) (1998) 2045.
12. K. KADONO, M. SHOJIYA, M. TAKAHASHI, H. HIGUCHI and Y. KAWAMOTO *J. Non-Cryst. Solids* **259** (1999) 39.
13. S. BUDDHUDU and F. J. BRYANT, *Spectrochemica Acta* **44A** (1988) 1381.
14. F. A. DAVIS and N. F. MOTT, *Philos. Mag*. **22** (1970) 903.
15. G. RACAH, *Phys. Rev*. **62** (1942) 438.
16. B. G. WYBOURNE, *J. Chem. Phys*. **32** (1960) 639.
17. E. Y. WONG, *ibid*. **35** (1961) 544.
18. Y. SUBRAMANYAM, Ph.D thesis, S.V. University, Tirupati, India, 1988.
19. R. REISFELD, *Structure and Bonding* (Berlin) **22** (1975) 123.
20. B. R. JUDD, *Phys. Rev.* **127** (1962) 750.
21. G. S. OFELT, *J. Chem. Phys*. **37** (1962) 511.
22. B. R. JUDD, *Proc. Phys. Soc*. London, Ser.A **69** (1956) 157.
23. W. T. CARNALL, H. CROSSWHITE and H. M. CROSSWHITE, "Energy Level structure and Transition Probabilities of Trivalent Lanthanides in LaF_3" Argonne National Laboratory Report, 1977.
24. R. D. PEACOCK, *Structure and Bonding* (Berlin) **22** (1975) 83.
25. J. HORMADALY and R. REISFELD, *J. Non-Cryst. Solids* **30** (1979) 337.
26. K. GATTERER, G. PUCKER, H. P. FRITZER and S. ARAFA, *ibid.* **176** (1994) 237.
27. M. B. SAISUDHA and J. RAMAKRISHNA, *Phys. Rev.* B **53** (1996) 6186.
28. E. W. J. L. OOMEN and A. M. A. VAN DONGEN, *J. Non-Cryst. Solids* **111** (1989) 205.
29. S. TANABE, T. OHAYAGI, N. SOGA and T. HANADA, *Phys. Rev B: Condens. Matter* **46** (1992) 3305.
30. S. TANABE, T. OHAYAGI, S. TODOROKI, T. HANADA and N. SOGA, *J. Appl. Phys*. **73** (1993) 8451.
31. R. J. MERINO, J. A. PARDO, J. I. PENA *et al.*, *Phys. Rev.*, B **56** (1997) 10907.
32. M. SHOJIYA, Y. KAWAMOTO and K. KADONO, *J. Appl. Phys*. **89**(9) 2001.
33. M. SHOJIYA, M. TAKAHASHI, R. KANNO *et al.*, *ibid*. **82** (1997) 6259.
34. L. RAMAMURTHY, T. S. RAO, K. JANARDHANAM and A. RADHAPATHY, *Spectrochemica Acta* Part A: **56** (2000) 1759.
35. H. TAKEBE, Y. NAGENO and K. MORINAGA, *J. Am. Chem. Soc.* **78** (1995) 116; erratum: 78, 2287.
36. J. V. SATHYANARAYANA, T. BALAJI, K. ANNAPURNA and S. BUDDHUDU, *Phys. Chem. Glasses*, **37** (1996) 41.

Received 14 August 2001
and accepted 29 October 2002